Jurnal
Teknologi

Full Paper

STUDY ON ADHESION STRENGTH OF TIN COATED BIOMEDICAL TI-13ZR-13NB ALLOY

A. Shah[a*], S. Izman[b], Siti Nurul Fasehah Ismail[c], Mas-Ayu H.[d], R. Daud[d]

[a]Faculty of Technical and Vocational, Universiti Pendidikan Sultan Idris, 35900 Tanjong Malim, Perak, Malaysia
[b]Faculty of Mechanical Engineering, Universiti Teknologi Malaysia, 81310 UTM Johor Bahru, Johor, Malaysia
[c]Faculty of Biosciences and Medical Engineering, Universiti Teknologi Malaysia, 81310 UTM Johor Bahru, Johor, Malaysia
[d]Faculty of Mechanical Engineering, Universiti Malaysia Pahang, 26300 Pekan, Pahang, Malaysia

Article history
Received
20 March 2017
Received in revised form
29 August 2017
Accepted
10 January 2018

*Corresponding author
armanshah@ftv.upsi.edu.my

Abstract

One of the crucial factors which determine the success of coated implantation and stability in the long run is the strength of adhesion between the coating and substrate. After implantation, a weakly adhered coating may delaminate and this might seriously restrict the implant's effectiveness and longevity. Based on past studies, the quality of TiN coating is directly influenced by the process parameters. The objective of this research is to evaluate the effect of N_2 gas flow rate on adhesion strength of biomedical grade Ti-13Zr-13Nb alloy. In this research, N_2 gas flow rate of 100, 200 and 300 sccm were varied while the other parameters (substrate temperature and bias voltage) were fixed. The scratch testing method was used to examine the adhesion strength of the TiN coating. This research used the calibrated optical images to verify the total coating failures on the scratched coated samples. The results indicated that the micro droplet form on the TiN coating decreases as the flow rate of the N_2 gas increases. In contrast, the TiN coating's adhesion strength increases with the increase of N_2 gas flow rate. It can be concluded that N_2 gas flow rate was significant factor in improving the coating properties of TiN on Ti-13Zr-13Nb alloy.

Keywords: Biomaterial, Ti-13Zr-13Nb, adhesion strength, TiN and CAPVD

Abstrak

Salah satu faktor yang penting dalam menentukan kejayaan salutan implan dan kestabilan untuk jangka masa panjang ialah kekuatan lekatan antara salutan dan substrat. Selepas proses implantasi, lekatan salutan yang lemah mungkin akan tertanggal dan ini akan memendekkan jangka hayat dan keberkesanan implan. Berdasarkan kajian lepas, kualiti salutan titanium nitrida secara langsung akan dipengaruhi oleh proses parameter. Objektif kajian ini ialah untuk menilai keberkesanan kadar aliran gas N_2 ke atas kekuatan lekatan gred bio-perubatan aloi Ti-13Zr-13Nb. Dalam kajian ini, kadar aliran gas nitrogen 100, 200 dan 300 sccm telah diubah manakala suhu substrat dan voltage bias telah dikekalkan. Ujian cakaran telah digunakan untuk menilai kekuatan salutan TiN. Selanjutnya, kajian ini menggunakan imej-imej optik ditentukur untuk mengesahkan jumlah kegagalan lapisan pada sampel bersalut yang dicakar. Keputusan kajian menunjukkan bahawa titisan mikro daripada lapisan TiN berkurang apabila kadar aliran gas N_2 bertambah. Sebaliknya, kekuatan lekatan salutan TiN akan bertambah dengan bertambahnya kadar aliran gas N_2.

Kata kunci: Biomaterial, Ti-13Zr-13Nb, kekuatan lekatan, TiN and CAPVD

1.0 INTRODUCTION

Titanium and its alloys are highly resistant to corrosion, have high strength-to-weight ratio, low elastic modulus and possess superior biocompatibility which make them extensively used as biomaterials [1-3]. However, the service lives of these alloys could be shortened due to their poor tribological properties, particularly when they are used for load bearing. Furthermore, titanium-based medical implants can generate wear debris, which causes toxicity and inherent implant failure [1, 2]. In this regard, one of the potential methods to increase tribological performance and mechanical properties of biomedical implants is surface treatment. Examples of commonly used surface treatment methods for treating biomedical implant are Chemical Vapour Deposition (CVD) [3], Physical Vapour Deposition (PVD) [4], Ion Implantation [5], Plasma Spray coating [6], Nitriding [7], and Thermal Oxidation [8]. Compared to other methods, the PVD technique has shown more encouraging results as it offers a lower processing temperature (<500 °C), over a varied coating thickness [9,10]. In this regard, the processing temperatures for other methods are relatively high and this limits the type of substrates, and causes unforeseen excessive residual stresses as well as phase transitions. Furthermore, medical implants with weakly adhered coating may delaminate after implantation, and this might severely compromise an implant's effectiveness and its life [11]. Consequently, past researches on TiN coating behaviour had documented aspects such as wear [12-14], corrosion resistance [15, 4, 12, 16] and fatigue test [17-19]. However, there are still limited studies on the behaviour of TiN coating behaviour on the strength of adhesion, particularly on the effects of PVD processing parameters. In this regard, Stallard *et al.* [20] used the magnetron sputtering technique to conduct a comparison between the adhesion strength of TiN coated Ti-6Al-4V alloy and steel when coating at the same conditions. Meanwhile, Kelly *et al.* [21] investigated the effects of pulsed DC power on both target and substrate, so that their impacts on the structural mechanical and tribological properties of TiN coatings could be ascertained. Gerth *et al.* [22] conducted an evaluation on metallic interlayers' (W, Mo, Nb, Cr, Ti, Ag and Al) influence on the adhesion of PVD TiN coatings on high-speed steels. Kataria *et al*. [23] performed different scratch modes of TiN coating on D9 steel while Mohseni *et al*. [24] investigated how substrate temperature of Ti/TiN affects the strength of adhesion. On the other hand, an analysis on the influence of deposition parameters the adhesion strength of TiN coating, which makes it more comprehensive compared to the aforementioned studies. Consequently, this current study used a reasonably new biomedical grade titanium (Ti-13Zr-13Nb), which was coated with micrometre thick TiN using the CAPVD.

2.0 METHODOLOGY

In this study, the biomedical grade Ti-13Zr-13Nb was used as the work piece material. This material was purchased with Marie Jay's metal. It has the chemical composition, as follows, in wt. %: Nb: 14; Zr: 13.5; Fe: 0.05; C: 0.04; N: 0.02; H: 0.002; O: 0.10 and Ti: balance. The material was cut into a disk, with the diameter of 10 mm x 2 mm of thickness. Prior to TiN coating, the substrates were first cleaned ultrasonically in acetone for an estimated 30 minutes, followed by a steam cleaning and finally dried using a stream of compressed air. Sand paper #320 was used to ground the substrates. This was done to provide the uniform initial surface roughness of 0.1 µm Ra. Then, the Ti-13Zr-13Nb was coated with TiN using CAPVD (Hauzer Techno Coating (HTC), with Europe BV 625/2 ARC). In these experiments, Titanium with purity level of 99.99% was used as the target. Before the deposition, metal ion etching was performed on the substrates for 5 minutes at the bias voltage of -1000V. Then, deposition process was conducted under these pre-determined parameters. First, the cathodic current was set at 100 A, the substrate bias was -125V and the temperature of the substrate was set at 300°C, and the substrate was deposited for 1 hour. In the meantime, the flow rate of nitrogen gas (100, 200 and 300 sccm) was the independent parameter and a Revetest scratch tester with the load range of 1-300 N was used to evaluate the TiN-coated substrates' adhesion strengths. The study also used a sphero-conical diamond with a 200 µm radius and 120° angle as an indenter. During scratching for a coating length of 5 mm, a consistent scratch speed of 1.13 mm/min and the load increment of 20 N/min were applied. Consequently, the friction coefficient and friction force graphs were used to determine the critical load for coating failure, and to confirm the scratch images captured using the optical microscope. Surface morphology and coating thickness were examined under SEM. An XRD was used to determine the crystalline structure. The analysis of microdroplets deposits on the coated samples was performed using Image J analyzer software.

3.0 RESULTS AND DISCUSSION

The researcher had deposited the TiN coating successfully on Ti-13Zr-13Nb at different nitrogen gas flow rates. As illustrated in Figure 1, there are crystal planes of the coated samples formed on the substrates at a range of nitrogen gas flow rates. This confirms that TiNs with a variety of crystal planes ((111), (200), (220), and (311)) were present on the substrates. Hence, it can be claimed that the film's textured growth with different planes have improved the coated samples' strength. It could also be observed that as the nitrogen gas flow rate increased from 100 to 300 sccm, the peak intensity of the (1 1 1) plane had decreased, whereas, regardless of substrate temperature, the intensity of the (2 0 0) plane had increased Kim *et al*. [25] reported the similar result which TiN coated glass substrate at a range of N_2 flow rates. Furthermore, compared with the N_2 flow rate of 100 sccm, the crystal plane (111) decrease was more apparent at the N_2 flow rates of 200 and 300 sccm. Thus, it is believed that the increase of PVD parameter from low to high polarity, affects the incident particles' kinetic energy onto the substrate surface. In this light, under these conditions, the growth orientation is affected by the competition between the surface and strain energies in TiN film.

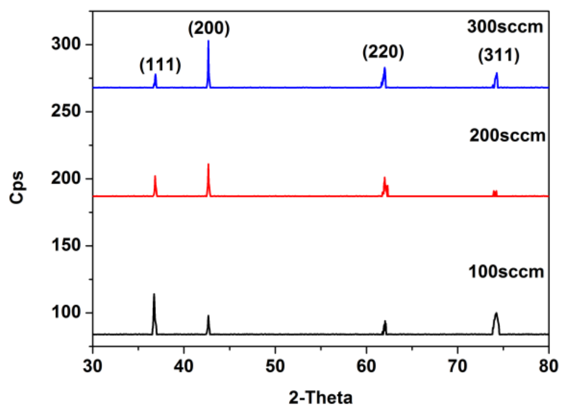

Figure 1 XRD patterns of TiN coating deposited at different nitrogen gas flow rate

Meanwhile, Figure 2 depicts how distinct flow rates of the nitrogen gas affected the surface morphology of TiN coated Ti-13Zr-13Nb alloy, regardless of the substrate temperatures. From this finding, it was observed that even though there is a smooth TiN coating spotted on the substrates, traces of white coloured micro droplets that resemble pin holes have also appeared, parallel to the observation by Mubarak *et al.* [26]. On the other hand, after TiN was deposited on the substrate, there are no evidences of grinding marks on the coating. From this observation, it can be concluded that the study's parameters are able to coat the grinding mark and improved the coated sample's surface morphology. In addition, as the nitrogen gas flow rate increased from 100 sccm to 300 sccm, the micro droplets that appeared on the substrates had been decreased and this resulted in a smoother looking surface. In this regard, micro droplets which was present in Figure 2 could be caused by the incomplete process of ionisation at a lower N_2 gas pressure.

Figure 3 shows the size distribution of the micro droplets, the total counts for N_2 gas flow rates. Figure 3 reveals that fewer micro droplets are observed with high N_2 flow rates. In other words, as N_2 flow rates increased, there were fewer micro droplets. The size of the micro droplets was smaller at higher N_2 flow rates.

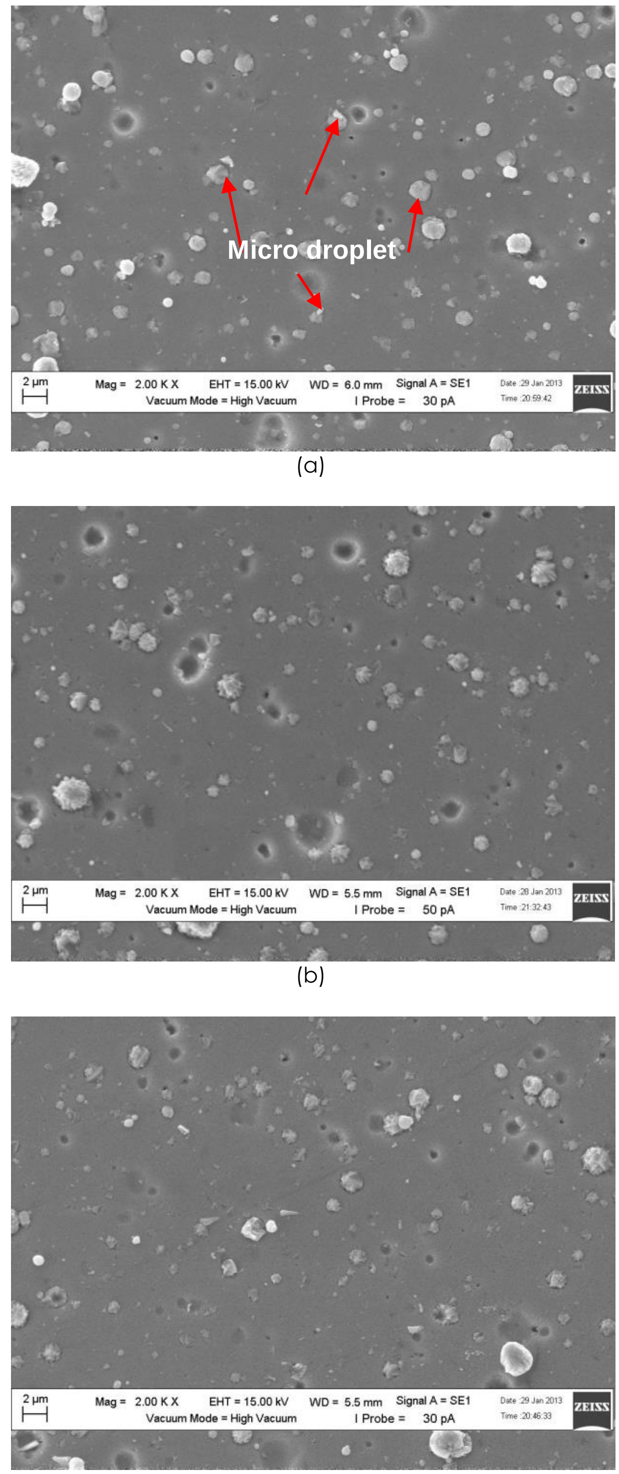

(a)

(b)

(c)

Figure 2 SEM Micrograph for TiN coated at different N_2 gas flow rate (a) 100 sccm (b) 200 sccm and (c) 300 sccm

These results indicate that the micro droplets between 0.5 to 1 µm dominate the surface of the substrates regardless of N_2 flow. The massive presence of micro droplets in Figure 2 can be attributed to incomplete ionization process at lower N_2 gas pressures.

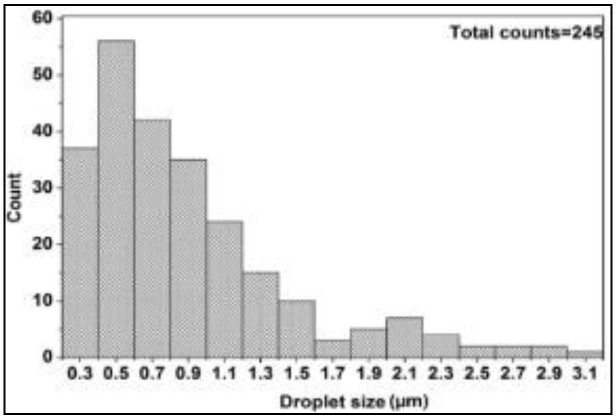

(a)

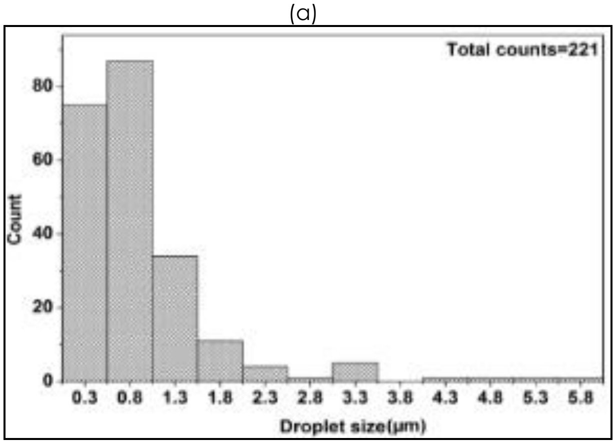

(b)

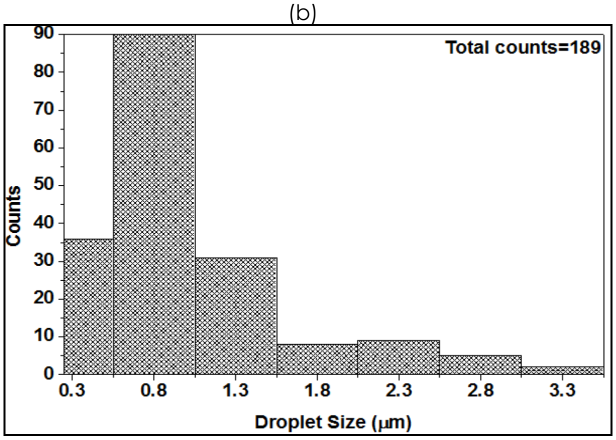

(c)

Figure 3 Size distribution of TiN coating micro droplets at N_2 flow rates (a) 100 sccm, (b) 200sccm, (c) 300 sccm

Image analysis software was used to verify the number of micro droplets on the TiN coating surface. Prior to counting the micro droplets, the images in Figure 2 were enhanced using a sharpened edge filter and Photoshop software to improve edge quality. This improved the contrast between the boarders of the micro droplets and the TiN coating matrix. A second image analysis software was employed to quantify and classify micro droplets features into average feret diameters and groups. This was completed by:

i) Selecting the region of interest;
ii) Image thresholding;
iii) Image calibration;
iv) Roundness adjustment; and
v) The quantification and grouping of macro droplets according to their size.

In the final step, only micro droplets larger than 0.2 µm were grouped. Any micro droplets smaller than 0.2 µm were regarded as noise. Well-defined micro droplets that fell in the acceptable range are represented using red and blue.

Cross sectional views of coated TiN at different N_2 flow rates are shown in Figure 4. All three conditions produced strongly adhered coatings with uniform thickness and without any noticeable voids or cracks in between the coating and the substrate. Even though a smooth coating was obtained, micro droplets still can be seen on the top layer of the coating. This phenomenon is quite common in CAPVD coating and widely reported by other researchers [27,28]. The coating thickness was measured using a cross sectional view. The thickness of the TiN coating at different parameters is summarized below in Figure 4.

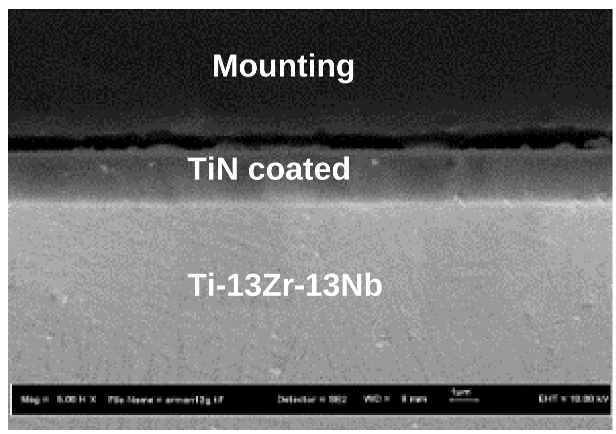

(a)

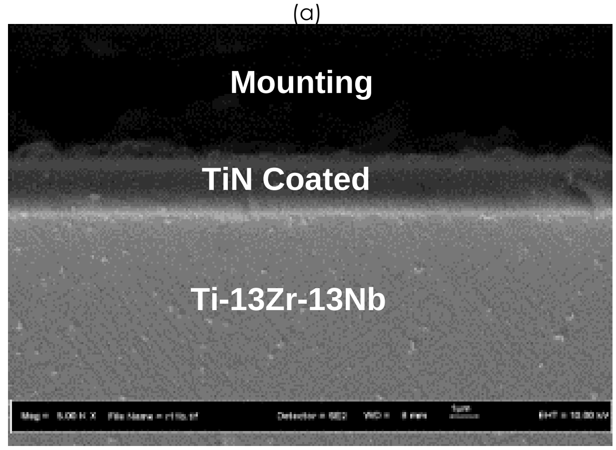

(b)

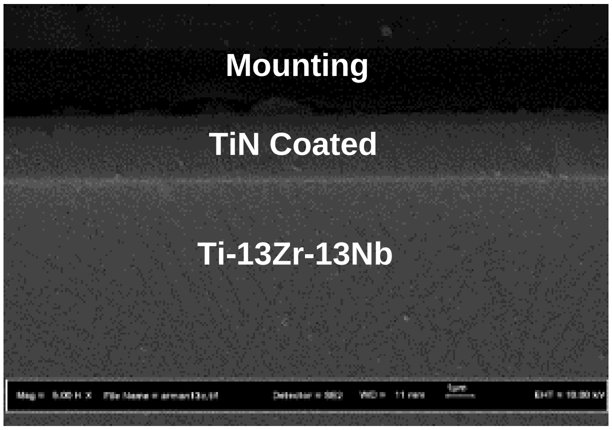

(c)

Figure 4 Cross section view of TiN after coating at different nitrogen gas flow (a) 100sccm, (b) 200sccm, (c) 300sccm

Figure 5 demonstrates that as N_2 flow rates increased, coating thickness also increased. By contrast, the coating was thinner when samples were coated at low N_2 flow rates. The effect of increasing the N_2 flow rates can be explained as follows: When N_2 flow rates increased, Ti metal ions become ionized and excited in the vacuum chamber and this provided a better chance for the metal ions to react with nitrogen gas to synthesis TiN. By contrast, lower N_2 flow rates limited the ionization process of Ti metal ions, reducing the synthesis of TiN and allowing a thinner coating to be deposited on the substrate.

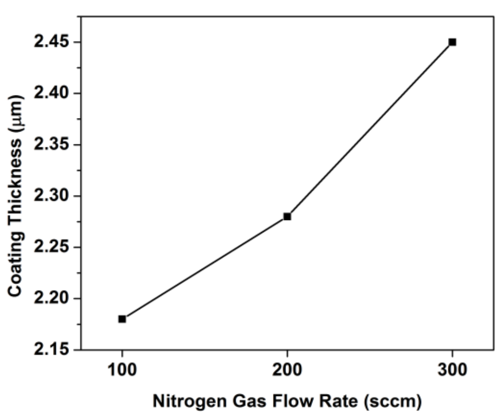

Figure 5 The effect of N_2 flow rates on coating thickness

The surface roughness of TiN coating at N_2 flow rates is shown in Figure 6. It demonstrates that surface roughness improved significantly as N_2 flow rates increased. Compared to low N_2 flow rates, the surface roughness looked rougher. The variations of surface roughness for N_2 flow rates 100, 200 and 300 sccm were the same. Less surface roughness was observed at when the N_2 flow rate was 300 sccm. The improvement on surface roughness was due to the decreasing of the number of micro droplets and grinding marks on the surface coating. Figure 2 confirms that the micro droplets on the surface and inconsistent substrate surfaces were due to micro droplets and pin holes that caused variations in surface roughness values.

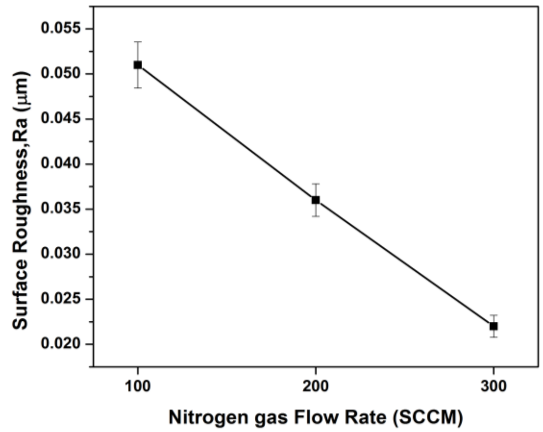

Figure 6 Effects of N_2 flow rates on surface roughness

At the same time, this study employed a series of scratch tests to assess the TiN coating's adhesion strength. These tests calculated the critical load needed to eliminate the coating from the substrate at a persistent speed with gradual load. Consequently, the gradual load applied in this experiment was adequate to delaminate the layers of TiN coating deposited on the Ti-13Zr-13Nb substrates. During the scratch tests, the researcher also plotted three graphs to record the changes in friction, friction coefficient and normal loads

Figure 7 shows the results when TiN layer was scratched on the Ti-13Zr-13Nb. The normal load graph indicates that for the load increment at constant 20 N/min during scratching, there was a linear increment for all conditions. Most of the time, this plot constantly appears in between the graphs of friction coefficient (top - red) and friction forces (bottom - purple). Consequently, the lack of acoustic sensor in the scratch tester system inspired the use of both friction coefficient and friction force graphs to ascertain the critical load that causes the coating failures. In this light, 22.5 to 28.6 N mark the critical load when the coating has failed. At the same time, the friction coefficient graphs for all conditions start with a value that ranges between 0.25 and 0.45, while the non-zero initial coefficient for friction values could be contributed by the resistance force which the indenter tip faced so that the roughness of the thin coating can be overcome, as shown in Figure 7. Therefore, the substrate surface of the tested coating had some micro droplets and pinholes, which might be caused by an ionise process which was incomplete during the deposition.

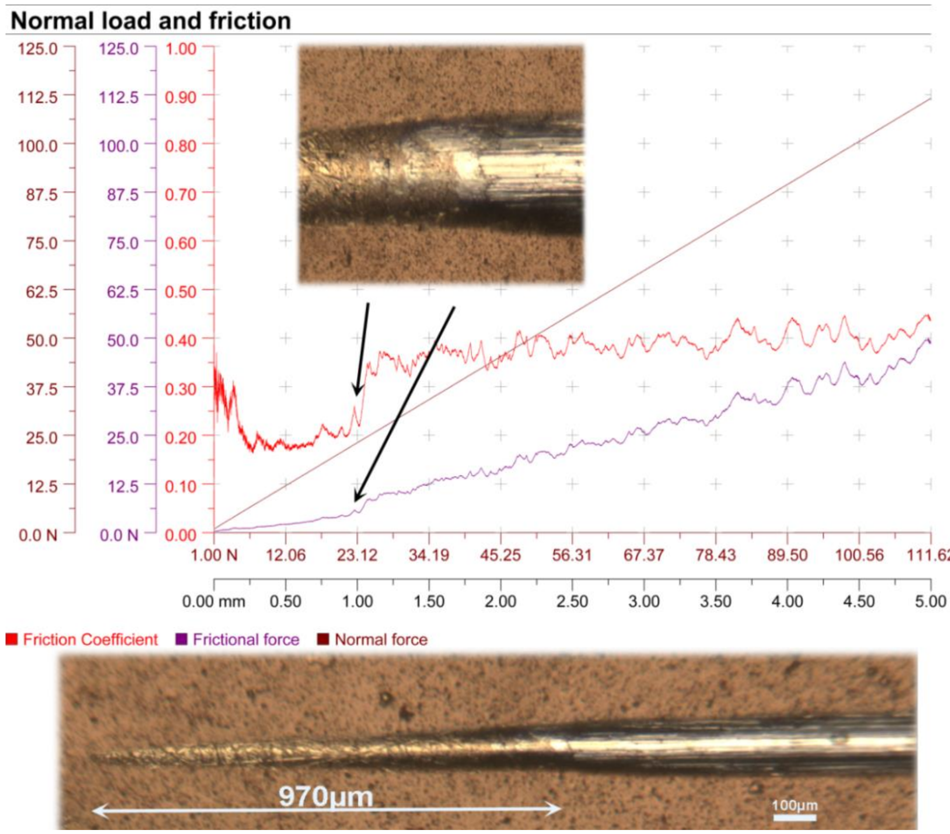
Normal load and friction
125.0
112.5
100.0
87.5
75.0
62.5
50.0
37.5
25.0
12.5
0.0 N
125.0
112.5
100.0
87.5
75.0
62.5
50.0
37.5
25.0
12.5
0.0 N
1.00
0.90
0.80
0.70
0.60
0.50
0.40
0.30
0.20
0.10
0.00
1.00 N 12.06 23.12 34.19 45.25 56.31 67.37 78.43 89.50 100.56 111.62
0.00 mm 0.50 1.00 1.50 2.00 2.50 3.00 3.50 4.00 4.50 5.00
Friction Coefficient
Frictional force
Normal force
970µm
100µm

(a)

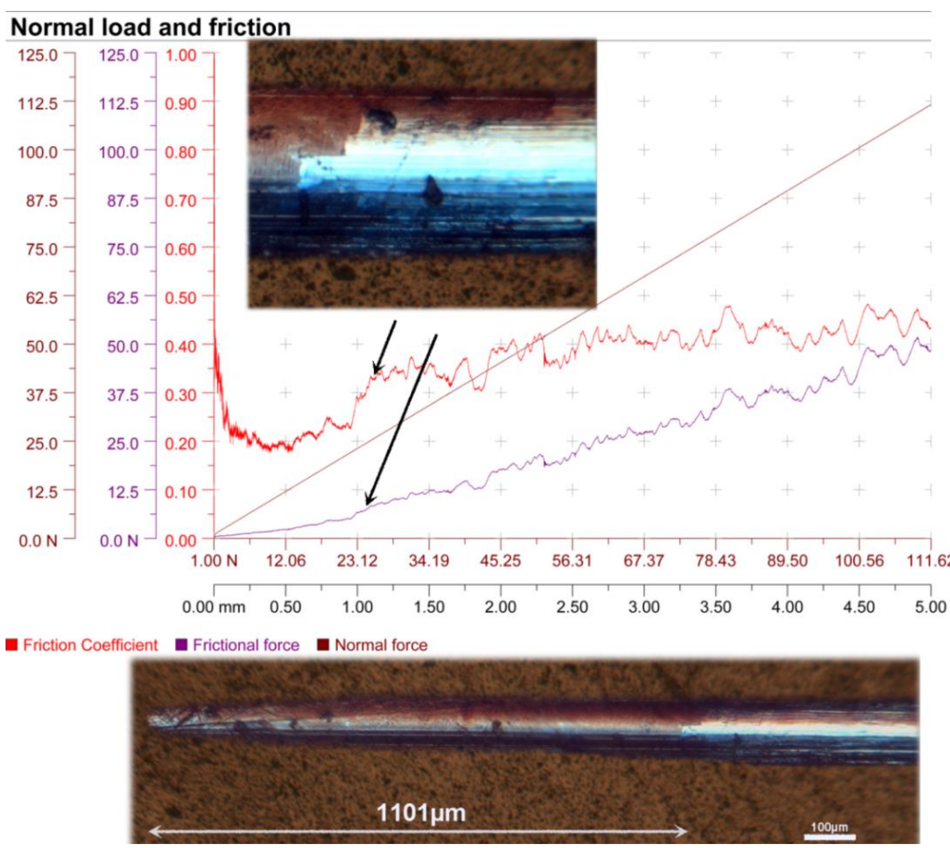
Normal load and friction
125.0
112.5
100.0
87.5
75.0
62.5
50.0
37.5
25.0
12.5
0.0 N
125.0
112.5
100.0
87.5
75.0
62.5
50.0
37.5
25.0
12.5
0.0 N
1.00
0.90
0.80
0.70
0.60
0.50
0.40
0.30
0.20
0.10
0.00
1.00 N 12.06 23.12 34.19 45.25 56.31 67.37 78.43 89.50 100.56 111.62
0.00 mm 0.50 1.00 1.50 2.00 2.50 3.00 3.50 4.00 4.50 5.00
Friction Coefficient
Frictional force
Normal force
1101µm
100µm

(b)

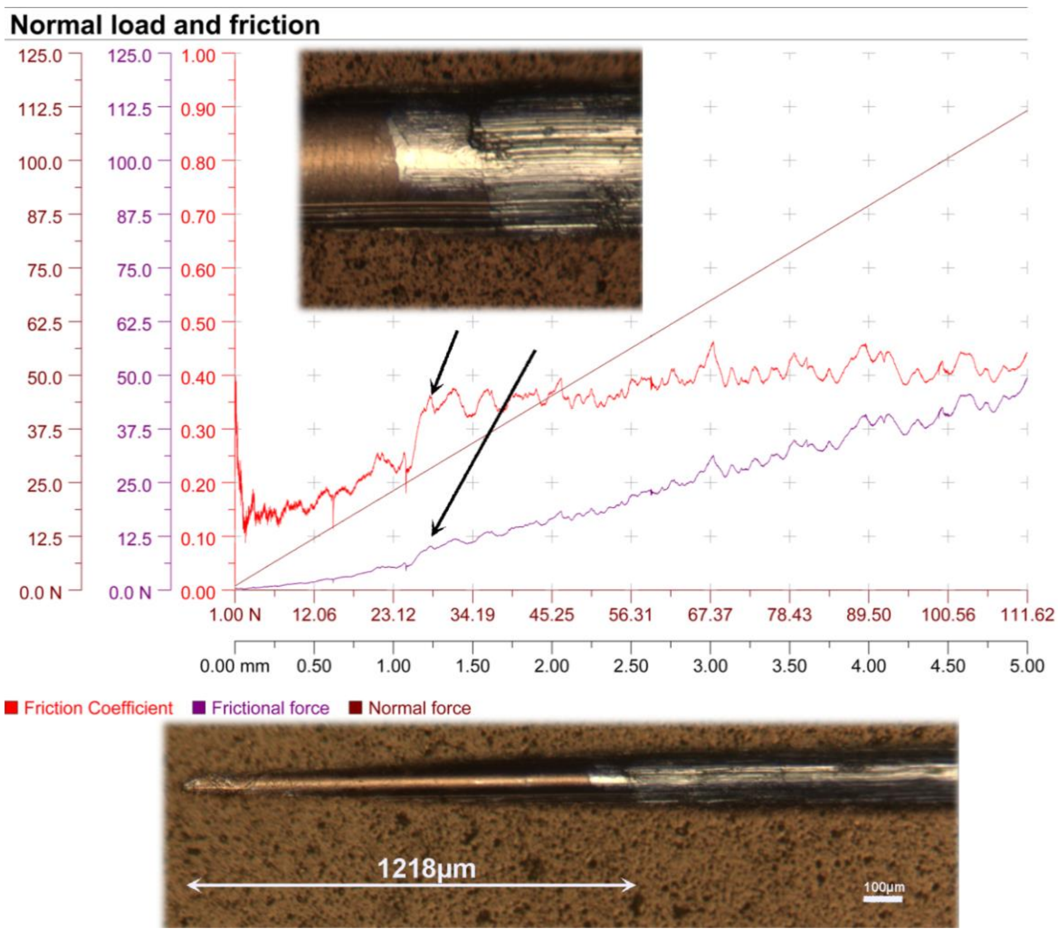

(c)

Figure 7 Optical images of scratch tracks along with graphs of friction coefficient, friction force and normal forces at (a) 100 sccm (b) 200sccm, (c) 300 sccm

On the other hand, even though there are evidences on the presence of coating defects on the substrates' surface, it is believed that the coating's adhesion strength is equivalent to the results of previous studies on Ti alloys [29-33].

A software was used to determine the critical load for coating failure. Here, a vertical line was positioned across the force graph of coefficient of friction and friction. The researcher had manually decided on the line position (total peel-off distance) based on both graphs' peak changes. In the meantime, since the graphs were not entirely transparent, determining the distance was challenging and to confirm the distance for the total failures, other optical images were captured on the scratched substrates to provide confirmation while the researcher used a-third party image analysis software to calculate the distance from the scratch to the substrate was completely stripped out of the coating. In this light, before the measurements are taken, calibrated ruler was used to calibrate the images. Figure 7 shows each of these respective graphs with these images attached while the arrows indicate the location of total coating failure occurrences.

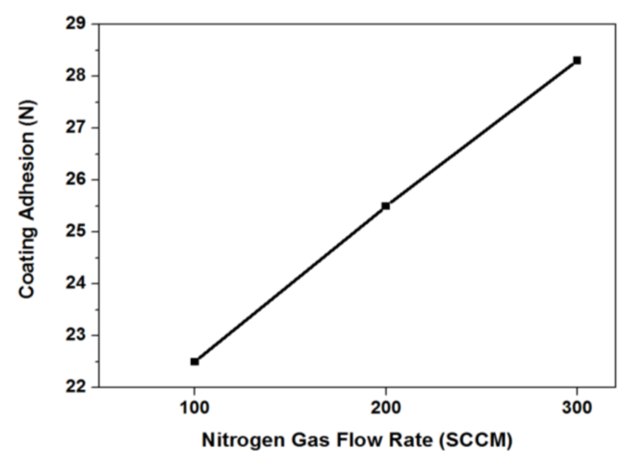

Figure 8 Critical load of TiN coated at various nitrogen gas flow rate

Figure 8 summarises the impacts of N_2 flow rates on critical loads. The conditions are the basis of plotted results. In general, as N_2 flow rates increases, he TiN coating's adhesion strength also increases, as illustrated by the higher critical load. Meanwhile, the highest adhesion strength (28.6 N) was evident on the substrate that had used extremely high coating conditions (300 sccm N_2 gas flow rates). Meanwhile, the substrate with the lowest adhesion strength (22.5 N) was the result of the use of severely low coating conditions (100 sccm gas flow rate). Hence, it can be concluded that the N_2 flow rates of 200 and 300 sccm had shown more significant results compared to N_2 flow rates of 100 sccm. Similar behaviour was reported by Berg *et al*. when they had studied the effects of N_2 gas flow rate of TiN coated on steel substrate [34]. Even with different types of coating and substrates, this behaviour still looked at the same phenomenon. The increasing of the adhesion at the higher N_2 flow rates had allowed more nitrogen plasma ions to penetrate the coating chamber. In this light, a higher chamber temperature increases the bombardment of energy as the substrate surface was struck by the nitrogen plasma. Consequently, the high bombardment energy accelerated the deposition process which leads to denser, thicker coating layers which are better adhered to the substrates. However, a contradiction was observed when severely low coating conditions were applied.

4.0 CONCLUSION

Using the CAPVD method, the TiN coatings have been successfully deposited on Ti-13Zr-13Nb. Hence, few main conclusions can be derived from this current investigation.

The study found that N_2 gas flow rate strongly influences the adhesion strength of TiN CAPVD coating. Thus, the deposition parameters' higher values led to better adhesion.

As the coated sample was deposited at the extreme high coating conditions (i.e. 300 sccm), the maximum critical load (28.5N) for the coated samples were obtained.

One crucial aspect to determine the adhesion strength and the smoothness of the coating is the initial surface roughness of the substrate. In this light, to obtain less friction and better adhesion, this study recommends surface roughness that is lower than 0.1µm Ra.

To determine the total coating failure, if the acoustic sensor is absent, calibrated optical images can also be utilised to confirm the critical load of the scratched samples.

Acknowledgement

The authors would like to express their highest gratitude to the Ministry of Higher Education and Universiti Pendidikan Sultan Idris (UPSI) for the funding of this research project (Fundamental Research Grant Schem FRGS) via code number 2016-0067-104-02. Special thanks to AMREC, SIRIM BERHAD and Universiti Malaysia Perlis (UniMAP) for providing their CAPVD coating and scratch testing facilities respectively.

References

[1] Geetha, M., Singh, A. K., Asokamani, R., Gogia, A. K. 2009. Ti Based Biomaterials, The Ultimate Choice for Orthopaedic Implants - A Review. *Progress in Materials Science*. 54(3): 397-425.

[2] Majumdar, P., Singh, S. B., Chakraborty, M. 2008. Wear Response of Heat-treated Ti-13Zr-13Nb Alloy in Dry Condition and Simulated Body Fluid. *Wear*. 264(11-12): 1015-1025.

[3] Polini, R., Barletta, M., Cristofanilli, G. 2010. Wear Resistance of Nano- and Micro-crystalline Diamond Coatings Onto WC-Co with Cr/CrN Interlayers. *Thin Solid Films*. 519(5): 1629-1635.

[4] Subramanian, B., Ananthakumar, R., Jayachandran, M. 2011. Structural and Tribological Properties of DC Reactive Magnetron Sputtered Titanium/Titanium Nitride (Ti/Tin) Multilayered Coatings. *Surface and Coatings Technology*. 205(11): 3485-3492.

[5] Luo, Y., Ge, S. 2009. Fretting wear Behavior of Nitrogen Ion Implanted Titanium Alloys in Bovine Serum Lubrication. *Tribology International*. 42(9): 1373-1379.

[6] Sathish, S., Geetha, M., Aruna, S. T., Balaji, N., Rajam, K. S., Asokamani, R. 2011. Sliding Wear Behavior of Plasma Sprayed Nanoceramic Coatings for Biomedical Applications. *Wear*. 271: 934-941.

[7] Cassar, G., Wilson, J. C. A.-B., Banfield, S., Housden, J., Matthews, A., Leyland, A. 2010. A Study of the Reciprocating-sliding Wear Performance of Plasma Surface Treated Titanium Alloy. *Wear*. 269(1-2): 60-70.

[8] Izman, S., Shah, A., Abdul-Kadir, M. R., Nazim, E. M., Anwar, M., Hassan, M. A., Safari, H. 2012. Effect of Thermal Oxidation Temperature on Rutile Structure Formation of Biomedical TiZrNb Alloy. *Advanced Material Research*. 393-395: 704-708.

[9] Shah, A., Izman, S., Fasehah, S. N. 2016. Study on Micro Droplet Reduction on Tin Coated Biomedical TI-13ZR-13NB Alloy. *Jurnal Teknologi*. 78(5-10): 1-5

[10] Shah, A., Izman, S., Hassan, M. A. 2016. Influence of Nitrogen Flow Rate in Reducing Tin Microdroplets on Biomedical TI-13ZR-13NB Alloy. *Jurnal Teknologi*. 78(5-10): 6-10.

[11] Lacefeld, W. R. 1999. Hydroxylapatite Coatings. In: L.L. Hench, J. L. Wilson (eds.). Introduction to Bioceramics. World Scientific Publishing Co.Pte.Ltd., London. 223-238.

[12] Sathish, S., Geetha, M., Pandey, N. D., Richard, C., Asokamani, R. 2010. Studies on the Corrosion and Wear Behavior of the Laser Nitrided Biomedical Titanium and Its Alloys. *Materials Science and Engineering: C*. 30(3): 376-382.

[13] Hoseini, M., Jedenmalm, A., Boldizar, A. 2008. Tribological Investigation of Coatings for Artificial Joints. *Wear*. 264(11-12): 958-966.

[14] Nolan, D., Huang, S.W., Leskovsek, V., Braun, S. 2006. Sliding Wear of Titanium Nitride Thin Films Deposited on Ti-6Al-4V Alloy by PVD and Plasma Nitriding Processes. *Surface and Coatings Technology*. 200(20-21): 5698-5705.

[15] Kim, W.-G., Choe, H.-C. 2012. Effects of TiN Coating on the Corrosion of Nanostructured Ti–30Ta–xZr Alloys for Dental Implants. *Applied Surface Science*. 258(6): 1929-1934.

[16] Subramanian, B., Jayachandran, M. 2008. Electrochemical Corrosion Behavior of Magnetron Sputtered TiN Coated Steel in Simulated Bodily Fluid and Its Hemocompatibility. *Materials Letters*. 62(10-11): 1727-1730.

[17] Choe, H. C., Lee, C. H., Jeong, Y. H., Ko, Y. M., Son, M. K., Chung, C. H. 2011. Fatigue Fracture of Implant System Using TiN and WC Coated Abutment Screw. *Procedia Engineering*. 10(0): 680-685.

[18] Vadiraj, A., Kamaraj, M. 2006. Characterization of Fretting Fatigue Damage of PVD TiN Coated Biomedical Titanium Alloys. *Surface and Coatings Technology*. 200(14-15): 4538-4542

[19] Vadiraj, A., Kamaraj, M. 2007. Effect of surface Treatments on Fretting Fatigue Damage of Biomedical Titanium Alloys. *Tribology International*. 40(1): 82-88.

[20] Stallard, J., Poulat, S., Teer, D. G. 2006. The Study of the Adhesion of a TiN Coating on Steel and Titanium Alloy Substrates Using a Multi-mode Scratch Tester. *Tribology International*. 39(2): 159-166

[21] Kelly, P. J., vom Braucke, T., Liu, Z., Arnell, R. D., Doyle, E. D. 2007. Pulsed DC Titanium Nitride Coatings for Improved Tribological Performance and Tool Life. *Surface and Coatings Technology*. 202(4-7): 774-780.

[22] Gerth, J., Wiklund, U. 2008. The influence of Metallic Interlayers on the Adhesion of PVD TiN Coatings on High-speed Steel. *Wear*. 264(9-10): 885-892.

[23] Kataria, S., Kumar, N., Dash, S., Ramaseshan, R., Tyagi, A. K. 2010. Evolution of Deformation and Friction During Multimode Scratch Test on TiN coated D9 Steel. *Surface and Coatings Technology*. 205(3): 922-927.

[24] Mohseni, E., Zalnezhad, E., Bushroa, A. R., Abdel Magid, H., Goh, B. T., Yoon, G. H. 2015. Ti/TiN/HA Coating on Ti–6Al–4V for Biomedical Applications. *Ceramics International*. 41(10, Part B): 14447-14457.

[25] Kim, H. T., Park, J. Y., Park, C. 2012. Effects of Nitrogen Flow Rate on Titanium Nitride Films Deposition by DC Facing target Sputtering Method. *Korean Journal of Chemical Engineering*. 29(5): 676-679.

[26] Mubarak, A., Hamzah, E., Toff, M. R. M. 2008. Study of Macrodroplet and Growth Mechanisms with and Without Ion Etchings on the Properties of TiN Coatings Deposited on HSS using Cathodic arc Physical Vapour Deposition Technique. *Materials Science and Engineering: A*. 474(1-2): 236-242.

[27] Krishnan, V., Krishnan, A., Remya, R., Ravikumar, K. K., Nair, S. A., Shibli, S. M. A., Varma, H. K., Sukumaran, K., Kumar, K. J. 2011. Development and Evaluation of Two PVD-coated β-titanium Orthodontic Archwires for Fluoride-induced Corrosion Protection. *Acta Biomaterialia*. 7(4): 1913-1927.

[28] Mubarak, A., Hamzah, E., Abbas, T., Toff, M. R. M., Qazil, I. A. 2008. Macrodroplet Reduction and Growth Mechanisms in Cathodic Arc Physical Vapor Deposition of Tin Films. *Surface Review and Letters*. 15(5): 653-659.

[29] Perry, A. J. 1981. Adhesion Studies of Ion-plated TiN on Steel. *Thin Solid Films*. 81(4): 357-366.

[30] Je, J. H., Gyarmati, E., Naoumidis, A. 1986. Scratch Adhesion Test of Reactively Sputtered Tin Coatings on a Soft Substrate. *Thin Solid Films*. 136(1): 57-67.

[31] Bull, S. J., Rickerby, D. S., Matthews, A., Leyland, A., Pace, A. R., Valli, J. 1988. The Use of Scratch Adhesion Testing for the Determination of Interfacial Adhesion: The Importance of Frictional Drag. *Surface and Coatings Technology*. 36(1-2): 503-517.

[32] Bull, S. J., Rickerby, D. S. 1990. Failure Modes in Scratch Adhesion Testing: Some Observations. In: T.S.S.a.D.G. Bhat (ed.). *Proceedings of the 3rd International Conference, Minerals, Metals and Materials Society, Warrendale*. 153-169.

[33] Farè, S., Lecis, N., Vedani, M., Silipigni, A., Favoino, P. 2012. Properties of Nitrided Layers Formed During Plasma Nitriding of Commercially Pure Ti and Ti–6Al–4V Alloy. *Surface and Coatings Technology*. 206(8-9): 2287-2292.

[34] Berg, G., Friedrich, C., Broszeit, E., Kloos, K.H. 1995. Comparison of Fundamental Properties of r.f.-sputtered TiNx and HfNx Coatings on Steel Substrates. *Surface and Coatings Technology*. 74-75 (PART 1): 135-142.